Development 137, 3551-3560 (2010) doi:10.1242/dev.047027

Oct1 regulates trophoblast development during early mouse embryogenesis

Vittorio Sebastiano[1,*,†], Mathieu Dalvai[2,*], Luca Gentile[1,*], Karin Schubart[2], Julien Sutter[1], Guang-Ming Wu[1], Natalia Tapia[1], Daniel Esch[1], Jin-Young Ju[1], Karin Hübner[1], Marcos Jesus Arauzo Bravo[1], Hans Robert Schöler[1,3], Fatima Cavaleri[1,‡,§] and Patrick Matthias[2]

SUMMARY

Oct1 (Pou2f1) is a transcription factor of the POU-homeodomain family that is unique in being ubiquitously expressed in both embryonic and adult mouse tissues. Although its expression profile suggests a crucial role in multiple regions of the developing organism, the only essential function demonstrated so far has been the regulation of cellular response to oxidative and metabolic stress. Here, we describe a loss-of-function mouse model for *Oct1* that causes early embryonic lethality, with *Oct1*-null embryos failing to develop beyond the early streak stage. Molecular and morphological analyses of *Oct1* mutant embryos revealed a failure in the establishment of a normal maternal-embryonic interface due to reduced extra-embryonic ectoderm formation and lack of the ectoplacental cone. *Oct1*$^{-/-}$ blastocysts display proper segregation of trophectoderm and inner cell mass lineages. However, Oct1 loss is not compatible with trophoblast stem cell derivation. Importantly, the early gastrulation defect caused by *Oct1* disruption can be rescued in a tetraploid complementation assay. Oct1 is therefore primarily required for the maintenance and differentiation of the trophoblast stem cell compartment during early post-implantation development. We present evidence that *Cdx2*, which is expressed at high levels in trophoblast stem cells, is a direct transcriptional target of Oct1. Our data also suggest that Oct1 is required in the embryo proper from late gastrulation stages onwards.

KEY WORDS: POU factors, Extra-embryonic ectoderm (ExE), Embryo patterning, Trophoblast stem (TS) cells, Mouse

INTRODUCTION

Oct1 (Pou2f1) belongs to the POU protein family (Veenstra et al., 1997), which historically included four transcription factors: the mammalian Pit1, Oct1 and Oct2 and *C. elegans* UNC-86. A common feature of the family is the POU domain, a bipartite DNA-binding motif consisting of two structurally independent subdomains, the POU-specific domain (POUs) and the POU homeodomain (POU_H), which are tethered by a linker of variable length ranging from 14 to 26 amino acids (Phillips and Luisi, 2000). The POU_S and POU_H domains bind independently, but in a cooperative manner, to each half-site of the target consensus. This modular structure operates as a single functional unit while conferring high DNA-binding affinity and specificity (Pomerantz and Sharp, 1994; Verrijzer et al., 1992). POU factors bind to the asymmetrical octamer canonical sequence ATGCAAAT and variants of this motif, and this has been shown to drive the expression of both ubiquitous and tissue-specific genes (Schöler, 1991). Most of the known POU proteins are temporally and spatially restricted during development. In accordance with their expression patterns, POU factors play pivotal roles in specific cell fate determination events. Oct6 (Pou3f1), for example, regulates Schwann cell differentiation (Jaegle et al., 1996), Brn3.2 (Pou4f2) controls retinal ganglion cell survival and differentiation (Erkman et al., 1996) and Oct2 (Pou2f2) has been implicated in the transcription of octamer-containing promoters, such as those of immunoglobulin genes in B cells (Muller et al., 1988; Scheidereit et al., 1987). To our knowledge, Oct4 (Pou5f1) is the only POU factor that has a role during early embryogenesis, when it is essential for the specification of a pluripotent inner cell mass (ICM) (Nichols et al., 1998) and for primordial germ cell survival (Kehler et al., 2004). Being ubiquitously expressed, Oct1 is an exception to the POU factor tissue-specific functionality. Oct1 activates the housekeeping genes encoding histone H2B and the U6 and U2 snRNAs (Hinkley and Perry, 1992; Segil et al., 1991; Yang et al., 1991), but it can also control transcription of *Pax6*, *Cdx2*, immunoglobulins and other tissue-specific genes, usually via interaction with cell-specific binding partners (Donner et al., 2007; Jin and Li, 2001; Mason et al., 1985; Strubin et al., 1995).

Development of an organism requires that cell fate is specified at the correct place and time in the embryo. The blastocyst is the first embryonic landmark in which lineage segregation is apparent, as it comprises cells of two different lineages. The ICM gives rise to the embryo proper and to the primitive endoderm, whereas the trophectoderm (TE) contributes only to extra-embryonic tissues. The proliferation and differentiation of extra-embryonic tissues is an absolute requirement for ensuring intra-uterine growth and survival of the embryo. The TE cells lining the blastocoel cavity (mural TE) differentiate after implantation into a layer of primary trophoblast giant cells, which are essential for promoting the exchange of nutrients and oxygen with the maternal uterine environment before the placenta has developed (Hemberger et al., 2003). The TE cells overlying the ICM (polar TE, or pTE) have a

[1]Max Planck Institute for Molecular Biomedicine, Department of Cell and Developmental Biology, Röntgenstrasse, 20 48149 Münster, Germany. [2]Friedrich Miescher Institute for Biomedical Research, Novartis Research Foundation, Maulbeerstrasse 66, 4058 Basel, Switzerland. [3]University of Münster, Faculty of Medicine, Domagkstraße 3, 48149 Münster, Germany.

*These authors contributed equally to this work
[†]Present address: Institute for Stem Cell Biology and Regenerative Medicine, Stanford School of Medicine, 1050 Arastradero Road, Palo Alto, CA 94304, USA
[‡]Present address: Institute for Stem Cell Research, University of Edinburgh, West Mains Road, Edinburgh EH9 3JQ, UK
[§]Author for correspondence (cavaleri@mpi-muenster.mpg.de)

Accepted 27 August 2010

high proliferative potential, and form the extra-embryonic ectoderm (ExE) and the ectoplacental cone (EPC) of the post-implantation embryo, which are inherently different with respect to growth potential. Only the pTE and the ExE harbor trophoblast stem (TS) cells, which depend on Fgf4 to proliferate, provided either by the adjacent ICM or epiblast (EPI). TS cells can also be cultured and expanded ex vivo in the presence of recombinant Fgf4 (Tanaka et al., 1998; Uy et al., 2002). By contrast, the EPC contains only differentiated diploid precursors that give rise to secondary giant cells and later on to the spongiotrophoblast layer of the placenta. Genetic studies have revealed that TE development and TS proliferation also depend on the endogenous expression of the transcription factors *Cdx2*, *Eomes* and *Elf5* (Donnison et al., 2005; Russ et al., 2000; Strumpf et al., 2005).

Besides being essential for placenta development, the ExE has an instructive role in patterning the embryo proper. The establishment of the proximal-distal (P-D) axis and its conversion into the anterior-posterior (A-P) axis depend on reciprocal and concerted interactions between the EPI, the visceral endoderm and the ExE, which ultimately lead to the formation of the anterior visceral endoderm (AVE) and the primitive streak (PS) at the prospective anterior and posterior sides of the embryo, respectively (Tam et al., 2006). The formation of both AVE and PS is intrinsically regulated by FGF, Bmp4, Nodal and Wnt signaling pathways (Tam et al., 2006; Thisse and Thisse, 2005).

Once the PS has been specified, cell delamination through the streak results in the formation of the mesoderm and the definitive endoderm. Proximal migration of the extra-embryonic mesodermal cells leads to expansion and then coalescence of the anterior and posterior amniotic folds into a single cavity, which is enclosed distally by the amnion and proximally by the chorion. By E8.5, the primitive body plan has been established and the allantois, which emerged as a finger-like structure where the PS first formed, expands upwards to make contact with the chorion. This embryonic stage marks the beginning of chorio-allantoic placenta formation and organogenesis.

As *Oct1* is expressed in pre- and post-implantation mouse embryos, we were interested in investigating the biological function of Oct1 during early development. A mouse model with severely hypomorphic *Oct1* alleles was generated previously (Wang et al., 2004). In a hybrid genetic background, a low level of *Oct1* expression has been reported to cause midgestation lethality due to decreased erythropoiesis and anemia. In primary embryonic fibroblasts derived from wild-type versus hypomorphic *Oct1* fetuses, total amounts of U2/U6 snRNAs and *H2B* transcripts were indistinguishable, although transfected octamer-driven reporter expression was affected by low Oct1 (Wang et al., 2004). In order to identify Oct1 function in fetal tissues other than the liver, expression profiling of *Oct1* hypomorphic and wild-type fibroblasts was undertaken. Even though this analysis revealed that Oct1 modulates genes that mediate cellular response to oxidative and metabolic stress (Shakya et al., 2009; Tantin et al., 2005), the question of whether, and how, Oct1 contributes to embryonic development remained unanswered.

Here, we have generated an *Oct1* loss-of-function mouse model by gene targeting. We show that *Oct1*-null mutant embryos display severe growth defects and die in utero at ~E7.0-8.0. We demonstrate that Oct1 primarily plays a novel and unexpected role in trophoblast development by ensuring TS cell maintenance and differentiation. We also provide evidence that the embryonic function of Oct1 is necessary to ensure development from the late gastrulation stage onwards.

MATERIALS AND METHODS

Generation of *Oct1* mutant mice and PCR genotyping of mice and embryos

Murine *Oct1* genomic sequences used in the construction of the *Oct1* targeting vector were derived from a mouse genomic lambda phage library, mapped and sequenced. A 6.3 kb *Kpn*I-*Bam*HI genomic fragment that includes the two exons encoding the POU_S domain was used as the 5′ homology arm, and a 0.89 kb *Xho*I-*Bgl*II genomic fragment derived from the intron sequence between the two exons encoding the POU_H domain was used as the 3′ homology arm. The homology arms were cloned on either side of a TK promoter-driven NeoR cassette. The targeting vector was linearized and electroporated into 129/Ola E14 embryonic stem (ES) cells. Correctly targeted G418-resistant clones were identified using a 735 bp *Bgl*II probe corresponding to the genomic POU_H domain, which detected a 2.3 kb wild-type and a 6.5 kb mutant fragment on Southern blots of *Hin*dIII-digested genomic DNA. Two of these ES cell clones were used for aggregation to C57BL/6 morulae, and the resulting chimeric mice were backcrossed to C57BL/6 animals to obtain germline transmission of the targeted allele.

Tail tips or embryos were digested in 100 mM Tris pH 8.0, 0.5% Tween 20, 0.5% NP40 and 0.1 mg/ml proteinase K at 55°C. The *Oct1* wild-type allele was detected by amplification of a 930 bp PCR product using primers specific for the POU genomic domain (see Table S1 in the supplementary material). The targeted *Oct1* allele was detected by amplification of a 980 bp product using primers specific for the inserted NeoR cassette and the POU genomic domain (see Table S1 in the supplementary material).

Tetraploid embryo aggregation experiments were conducted as previously described (Eakin and Hadjantonakis, 2006).

Cell culture and immunofluorescence

ES and TS cells were derived and grown under standard conditions (Cavaleri et al., 2008; Tanaka et al., 1998). ES and TS cells were processed for immunostaining as previously described (Cavaleri et al., 2008). Antibodies and dilutions were: anti-SSEA-1 (Developmental Studies Hybridoma Bank, MC-480) 1:200; anti-Oct1 (Santa Cruz, C-21) 1:50; and anti-Cdx2 (BioGenex, Cdx2-88) 1:500.

Histology and in situ hybridization (ISH)

Pregnant females were dissected at the indicated gestational age, counting noon of the day of the vaginal plug as E0.5. For embedding, deciduae were fixed overnight in 4% paraformaldehyde and processed for routine paraffin histology. Whole-mount RNA ISH was performed as described for high-background probes (Zeller et al., 2001). After signal detection, embryos were photographed and genotyped by PCR. Antisense riboprobes were synthesized using a DIG RNA Labeling Kit (Roche) according to the manufacturer's instructions.

Electrophoretic mobility assay (EMSA) and western blotting

EMSA for spleen, thymus and ES whole-cell extracts was performed as described (Sauter and Matthias, 1998). In brief, radioactively labeled DNA fragments containing an octamer site from the IgH chain enhancer were used as probe. The fragments were labeled with [γ-^{32}P]ATP and polynucleotide kinase. Binding reactions (20 μl) were set up with 2 μg whole-cell extract, 10,000 cpm of probe, 1 μg poly(dI-dC) and 1 μg denatured herring sperm DNA in the binding buffer (4% Ficoll 400, 20 mM HEPES pH 7.9, 50 mM KCl, 1 mM EDTA, 0.25 mg/ml bovine serum albumin). After 10 minutes incubation at room temperature, samples were electrophoresed in 4% polyacrylamide gels in 0.25×TBE. The gel was dried and exposed to a phosphorimager screen for quantification.

For western blotting, cells were lysed in 2× Laemmli buffer, vortexed for 3 seconds, heated at 99°C for 10 minutes and centrifuged for 5 minutes at 16,000 ***g*** at 4°C. Then 12.5-25 μl of lysate were electrophoresed on an 18% polyacrylamide minigel under denaturing SDS-PAGE conditions. Proteins were transferred to a PVDF Immobilon membrane (Millipore, Schwalbach, Germany) and processed for immunodetection with ECL Plus reagents (GE Healthcare, Solingen, Germany). Antibodies and dilutions were: anti-Oct1 (Santa Cruz, C-21) 1:1000; and anti-β-actin (Actb) (Abcam, 8226) 1:5000.

Quantitative expression analysis

For real-time analysis of gene expression, embryos (or cells) were harvested and processed as previously described (Boiani et al., 2003). Briefly, single E3.5 or E6.5 embryos were lysed in RLT buffer (Qiagen, Hilden, Germany), and 50% or 20% of the lysate was used for genomic DNA purification; the remaining lysate was used for RNA extraction. Complementary DNA synthesis was performed with the High Capacity cDNA Archive Kit (Applied Biosystems, Darmstadt, Germany) following the manufacturer's instructions. Transcript levels were determined using ABI PRISM Sequence Detection System 7900HT (Applied Biosystems) and the ready-to-use 5′-nuclease Assays-on-Demand as follows: *Oct1*, Mm00448332_m1; *Cdx2*, Mm00432449_m1; *Esrrb*, Mm00442411_m1; *Eomes*, Mm01351984_m1; *Fgfr2*, Mm00438941_m1; *Oct4*, Mm00658129_gH; *Hand1*, Mm00433931_m1; *Hprt1*, Mm00446968_m1. Quantification was normalized to the endogenous *Hprt1* gene using the ΔΔCt method (ABI Prism 7700 Sequence Detection System User Bulletin #2, relative quantification of gene expression).

Chromatin immunoprecipitation assay (ChIP)

ChIP assays were performed following the manufacturer's recommendations (Agilent mammalian ChIP-on-chip protocol), with a few modifications: the number of cells used for each experiment was reduced to 1×10^6, and the amount of DNA used for each immunoprecipitation was of 1×10^5 cell equivalents. Briefly, cells were cross-linked and their nuclei were pelleted and lysed. After sonication, DNA was used to amplify the human/mouse reference gene *ACTB*/*Actb* to equalize the input used for the immunoprecipitation step. G protein-conjugated Dynabeads (25 μl; Invitrogen) were coupled with 10 μg of a polyclonal antibody directed against the mammalian Oct1 protein (Santa Cruz, C-21) and mixed with the sonicated DNA. Following overnight incubation, the beads were washed and the DNA eluted accordingly to the Agilent protocol.

Quantitative (q) PCR was used to determine the amount of immunoprecipitated DNA. Normalization and quantification were carried out as previously described (Johnson et al., 2002) using the ΔΔCt method relative to the control gene *ACTB*/*Actb*. Input control was used to determine the linear dynamic range and the efficiency of each qPCR reaction. The regions including the putative Oct1 binding consensus (human, –117 bp; mouse, –154 bp; relative to the transcription start site) and two regions more than 600 bp distant therefrom were amplified from human/mouse *CDX2*/*Cdx2* loci with specific primers (see Table S1 in the supplementary material).

Vector construction, lentiviral particle production and TS cell infection

DNA constructs designed to produce short hairpin (sh) RNAs targeting *Oct1* (5′-GCATCTAGCCCAAGTGCTTTGTTCAAGAGACAAAGCACTTGGGCTAGATGC-3′) or *lacZ* (5′-GTGGATCAGTCGCTGATTAAATTCAAGAGATTTAATCAGCGACTGATCCAC-3′) were cloned in front of the H1 promoter in the pLVTHM vector to produce pLVTHM-shOct1 and pLVTHM-shlacZ, respectively. pLVTHM-Td-tomato was constructed from pLVTHM by replacing the GFP with the Td-tomato coding sequence. pLVTHM-Oct1-2A-tomato was generated by introducing the Oct1 coding sequence and the 2A peptide in frame with Td-tomato. PLVTHM-wtCdx2 and pLVTHM-mutCdx2 were constructed by replacing the EF1α promoter in pLVTHM with the wild-type *Cdx2* promoter (–154 to +126) or the *Cdx2* promoter containing a mutated Oct binding site (CTGCAGAT) (Jin and Li, 2001), respectively.

The recombinant lentiviral particles were produced by transient transfection of 293T cells with 12 μg of each viral vector, 8.5 μg psPax2 and 3 μg pMD2.G using Lipofectamine 2000 (Invitrogen) according to the manufacturer's instructions. The supernatant was collected after 48 hours and concentrated by ultracentrifugation at 26,000 rpm (80,000 ***g***) for 2 hours at 4°C using an SW41 rotor (Beckman Coulter). After ultracentrifugation, the supernatant was decanted and the viral pellet was resuspended in 200 μl Dulbecco's Modified Eagle Medium. The suspension was stored at –80°C until use. Eight thousand TS cells were plated on gelatin in 4-well plates and 24 hours later 20 μl of the concentrated virus was added to the medium. Cells were washed after 16 hours of incubation and transferred onto mouse embryonic fibroblasts (MEFs).

Oct1 knockdown and transactivation assay

Feeder-free TS cells were infected with pLVTHM-shOct1 or pLVTHM-shlacZ and sorted for GFP expression 48 hours after being plated on MEFs. GFP^+ TS cells were lysed in RLT buffer (Qiagen) and reverse-transcribed using the High-Capacity cDNA Archive Kit (Applied Biosystems) following the manufacturer's instructions. The expression of *Oct1* and *Cdx2* was determined using the ABI PRISM Sequence Detection System 7900HT (Applied Biosystems) and the ready-to-use 5′-nuclease Assays-on-Demand (see above).

TS cells, co-infected with pLVTHM-Oct1-2A-tomato and either PLVTHM-wtCdx2 or pLVTHM-mutCdx2, were sorted for Td-tomato and GFP expression 48 hours after being plated on MEFs. Td-tomato and GFP mean fluorescence intensities were measured using FACSdiva software (BD Biosciences).

RESULTS

Inactivation of the mouse *Oct1* gene

To assess the role that Oct1 plays during embryogenesis we inactivated the mouse *Oct1* locus by homologous recombination in ES cells. At least four (multiple) alternatively spliced isoforms of *Oct1* have been identified in mice (Zhao et al., 2004). These isoforms have a unique 3′ terminus and a common 5′ moiety with an intact POU binding domain. Wang and colleagues previously attempted to disrupt *Oct1* by replacement of exon 3 with a neomycin cassette (Wang et al., 2004). This gene targeting strategy was intended to lead to the production of transcripts harboring a frameshift mutation that upon translation would result in the deletion of two-thirds of the Oct1 polypeptide. However, owing to the utilization of translation initiation sites downstream of exon 3, residual Oct1 binding activity was detected with nuclear extracts isolated from *Oct1* double-targeted MEF cells. Therefore, the engineered *Oct1* mutation was considered to constitute a severely hypomorphic allele. We thus decided to inactivate the *Oct1* locus by replacing exon 11, which encodes the linker domain and the 5′ terminus of the POU_H domain, with the neomycin resistance gene (Fig. 1A). Properly targeted ES clones were identified by Southern blotting of *Hin*dIII-digested genomic DNA (Fig. 1B).

Transcripts from the targeted allele were expected to contain exon 10 spliced to exon 12 and hence a nonsense mutation that would lead to the translation of a C-terminally deleted Oct1 protein unable to bind DNA. In order to characterize the splicing events occurring at the targeted allele, reverse transcription PCR was performed with RNA extracted from wild-type, heterozygous and null *Oct1* embryos. A DNA fragment corresponding to the expected length for an exon 10 to exon 12 splicing event was obtained from cDNA samples of heterozygous and null genotypes with an oligo pair specific to exons 9 to 13, whereas no amplification product was obtained with cDNA isolated from null embryos when an oligo pair specific to exons 9 to 11 was used (Fig. 1C). Sequence analysis confirmed the amplification product of the mutant *Oct1* cDNA.

We then investigated the binding activity of the mutant Oct1 protein by performing EMSA experiments with nuclear extracts isolated from both spleen and thymus cells from mice heterozygous for the *Oct1* mutation. Besides the endogenous Oct protein complexes formed with wild-type extracts, no additional complex that could indicate a residual binding capability of the truncated Oct1 protein was detected in the presence of heterozygous spleen or thymus cell extracts (Fig. 1D). Furthermore, quantification of the EMSA fluorograms showed that the spleen or thymus cells of heterozygous mice contain approximately half of the wild-type Oct1 binding activity (Fig. 1E). Taken together, these results

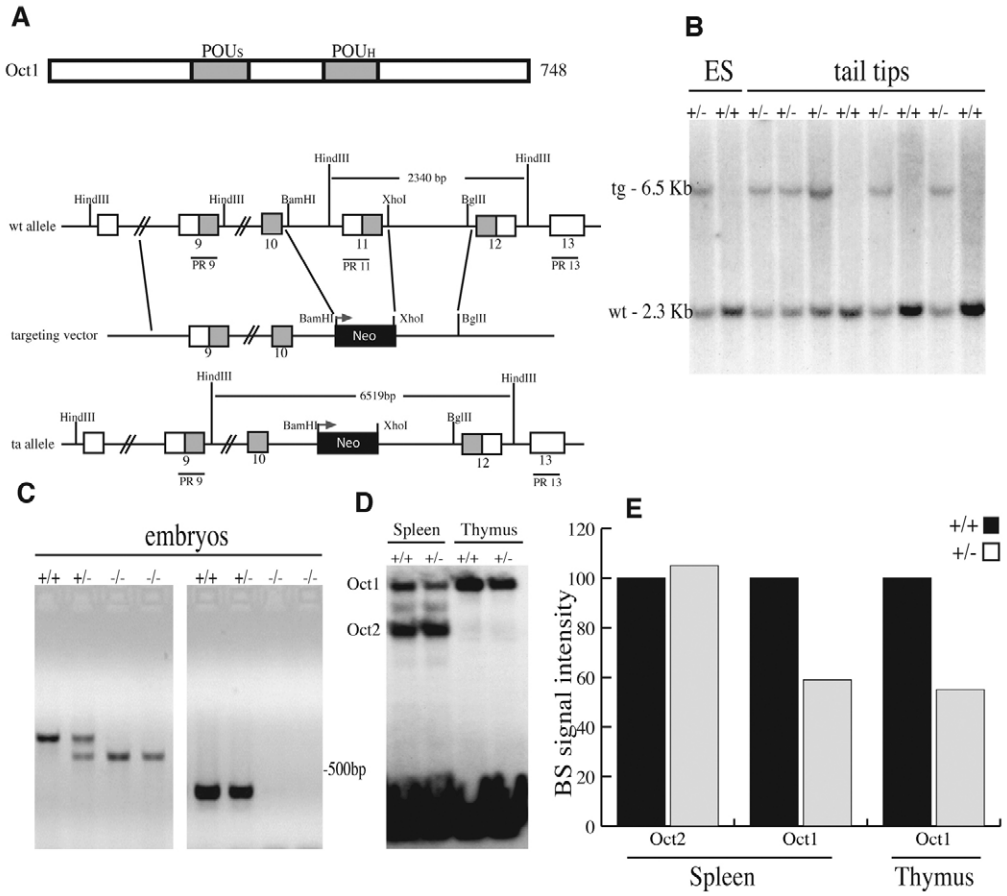

Fig. 1. Inactivation of the mouse *Oct1* locus. (**A**) Schematic representation of Oct1 protein (top), the *Oct1* (*Pou2f1*) genomic locus (wild-type, wt) and of the targeting vector used to generate the null allele (ta). (**B**) Southern blot analysis of genomic DNA derived from wild-type and *Oct1*-heterozygous ES cells or mice after digestion with *Hin*dIII. Transgenic (tg) band, 6.5 kb; wild-type band, 2.3 kb. (**C**) RT-PCR performed with primer sets for *Oct1* exon 9, 11 and 13 sequences. Amplification from wild-type and mutated cDNAs with primers specific for exons 9 and 13 (lanes 1-4) gives two different products; amplification with primers specific for exons 9 and 11 (lanes 5-8) amplifies the wild-type cDNA only. Position of the primers (PR) used is outlined in A. (**D**) Electrophoretic mobility assay (EMSA) of a radioactively labeled octamer motif (ATGCAAAT) with 2 μg of whole-cell extracts from spleen and thymus of wild-type and *Oct1*-heterozygous mice. In the spleen, the B cell-specific Oct2 and Oct1 bind to the octamer probe. In the thymus, Oct1 is the only octamer-binding protein. (**E**) Quantification of the EMSA results. The bandshift (BS) signal intensity from Oct complexes in wild-type extracts (black bars) was set to 100%. The ratios between the signal intensities from the complexes in heterozygous (white bars) and wild-type extracts are given as percentages.

indicate that our *Oct1* targeted allele results in the production of a non-functional, truncated Oct1 protein that is unable to bind DNA, and can thus be regarded as a null allele.

Loss of Oct1 causes early embryonic lethality

Heterozygous *Oct1* mice derived from two independent ES cell clones appeared normal and fertile. However, no viable $Oct1^{-/-}$ pups were recovered from intercrossing heterozygous animals. To assess the time frame of embryonic lethality, deciduae from heterozygote matings were dissected at various stages of gestation and isolated embryos were genotyped. $Oct1^{-/-}$ embryos were recovered at E6.5 at the expected Mendelian ratio (Table 1). However, the frequency with which viable mutant embryos were recovered decreased from E7.5, and at E9.5 only resorbed null embryos were found, suggesting that mutant embryos die between E7.5 and E9.0. Morphological examination of embryos at ~E7.5 revealed that $Oct1^{-/-}$ embryos were oval or asymmetric in shape and showed no evident demarcation between the embryonic and the extra-embryonic regions (Fig. 2A). They appeared developmentally arrested and resembled egg cylinders with a pro-amniotic cavity, whereas their littermates had developed up to late-streak stage and consequently displayed proper separation of the amniotic and exocoelomic cavities, as marked by chorion and amnion formation (Fig. 2A).

In order to identify possible defects at the tissue and cellular levels we performed in utero histological analysis of *Oct1* littermates. Since we were unable to genotype concepti from sectioned deciduae, we attributed a null genotype to concepti that showed no obvious P-D polarity. At E7.0, presumptive *Oct1*-null

Table 1. Genotypic analysis of progeny from *Oct1* heterozygous intercrosses

		n (%)			
Stage	Total*	$Oct1^{+/+}$	$Oct1^{+/-}$	$Oct1^{-/-}$	Mutant phenotype
E6.5	44	11 (25.0)	23 (52)	10 (23)	Small
E7.5	47	14 (29.7)	26 (55.3)	7 (15.0)	Severely delayed
E8.5	53	14 (26.4)	33 (62.2)	6 (11.4)	Severely delayed
E9.5	31	10 (32.2)	18 (58.1)	3 (9.7)	Disintegrating

*Total number of embryos typed.

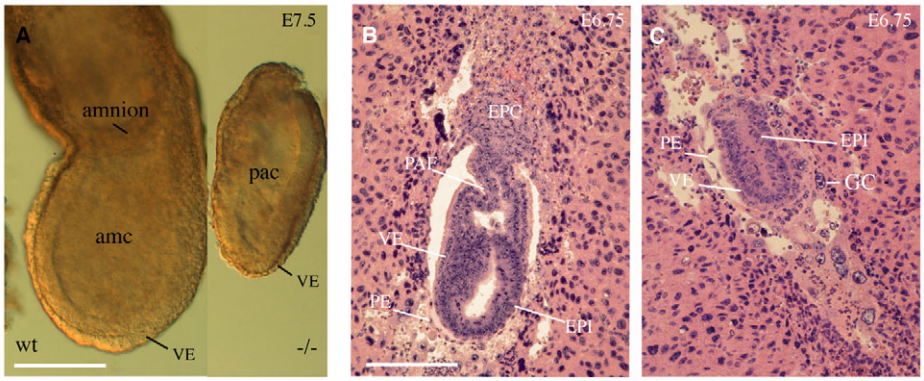

Fig. 2. Morphological and histological defects in *Oct1* mutant embryos. (**A**) *Oct1*$^{-/-}$ mouse embryos are smaller than wild-type littermates at E7.5. The amniotic and exocoelomic cavities are readily distinguishable in the wild-type embryo, whereas the *Oct1* mutant littermate can be recognized by the presence of the pro-amiotic cavity only. (**B**,**C**) Hematoxylin and Eosin-stained sagittal sections of E6.75 littermates, showing a complete lack of the EPC in the presumptive *Oct1*$^{-/-}$ embryo (C), which, by contrast, is clearly detectable in the wild-type counterpart (B). amc, amniotic cavity; pac, pro-amniotic cavity; VE, visceral endoderm; EPC, ectoplacental cone; PAF, posterior amniotic fold; PE, parietal endoderm; EPI, epiblast; GC, giant cell. Scale bars: 150 μm in A; 200 μm in B,C.

mutant embryos appeared reduced in size and lacked a structured EPC, which had invaded the maternal endometrium, although primary giant cells were visible around the conceptus (Fig. 2C). By contrast, the outer epithelial layers of parietal and visceral endoderm did not display any obvious defect (Fig. 2B,C). These results suggest that Oct1 might be crucial for the establishment of a proper embryonic-maternal interface that ensures embryo development before placenta formation takes place.

Oct1-null embryos are defective in trophoblast development

In order to investigate the molecular basis of the early post-implantation lethality caused by Oct1 deficiency, we examined the expression of lineage-specific molecular markers by whole-mount ISH.

Nodal, the Nodal co-receptor Cripto (Tdgf1 – Mouse Genome Informatics), Otx2 and Oct4 are expressed in the EPI of pregastrulating embryos. Nodal and Cripto become restricted to the posterior EPI as gastrulation commences at E6.5 (Brennan et al., 2001; Ding et al., 1998). In *Oct1* mutant embryos, as in the wild type, *Nodal* transcripts were found in a proximal-to-distal distribution and predominantly on the posterior side of the embryo (Fig. 3A). Expression of *Cripto* was also unaltered in *Oct1*-null embryos (Fig. 3B). At E6.5 and E7.75, *Oct1* mutant embryos displayed a strong and almost ubiquitous pattern of *Otx2* and *Oct4* expression, respectively, whereas wild-type and heterozygous littermates showed the correct distal pattern (Fig. 3C,D). These results suggest that *Oct1*-null embryos are mainly composed of embryonic ectoderm surrounded by visceral endoderm and might lack proximal extra-embryonic tissues.

We then probed embryos for extra-embryonic markers. *Bmp4* and the caudal-related homeobox gene *Cdx2* are expressed within the proximal region of the ExE (pExE) immediately adjacent to the EPI of E6.5 embryos (Beck et al., 1995; Lawson et al., 1999). *Eomes* (Russ et al., 2000), the nuclear orphan receptor *Esrrb* (Luo et al., 1997), the fibroblast growth factor receptor *Fgfr2* (Haffner-Krausz et al., 1999), *Pace4* (*Pcsk6* – Mouse Genome Informatics) (Donnison et al., 2005) and *Bmp8b* (Ying and Zhao, 2000) mark the whole ExE of early gastrulating embryos, with *Fgfr2* and *Bmpb8b* also being expressed in the EPC.

Bmp4 expression was consistently found at the proximal pole of *Oct1* mutant embryos (Fig. 3E). By contrast, *Cdx2* transcripts could not be detected in null embryos. However, because the intensity of the signal obtained with the *Cdx2* probe used was relatively weak, we cannot exclude the possibility that the level of *Cdx2* expression was just below our limit of detection (Fig. 3F). qRT-PCR analysis of wild-type, heterozygous and null *Oct1* E6.75 embryos confirmed the above interpretation of the *Cdx2* ISH data, and showed downregulation of *Cdx2*, *Esrrb* and the pan-trophoblastic marker *Hand1* (Cross et al., 1995) (see Fig. S1 in the supplementary material). *Eomes*, *Fgfr2* and *Pace4* were transcribed in *Oct1*-null embryos, although in a significantly reduced domain compared with their wild-type or heterozygous counterparts (Fig. 3G-I). Surprisingly, *Bmp8b* could not be detected in *Oct1*-null embryos (Fig. 3I). These results indicate that only an ExE-like compartment that is severely compromised in size can form in the absence of Oct1. We then investigated the expression of the Achaete-scute homolog *Mash2* (*Ascl2* – Mouse Genome Informatics), which is a marker of the diploid precursors of the ExE/EPC transition tissue and of the EPC at early gastrulation stages (Guillemot et al., 1994). *Mash2* transcripts were absent in *Oct1*-null embryos (Fig. 3L). Collectively, these results suggest that loss of Oct1 activity affects ExE development and impedes EPC formation.

Oct1 loss leads to ectopic AVE formation

Embryo patterning has been shown to be largely dependent on the reciprocal interaction between ExE and EPI. Since Oct1 deficiency compromised ExE development, the next step was to determine whether the embryo body plan was correctly established in *Oct1*-null embryos. To this end, we examined AVE and PS formation.

AVE cells express both *Lim1* and *Hex* (*Lhx1* and *Hhex*, respectively – Mouse Genome Informatics) at early to mid-gastrulation stages (Thomas et al., 1998; Tsang et al., 2000). Additionally, *Lim1* marks the PS and nascent mesodermal cells migrating away from the streak, whereas *Hex* marks cells of nascent definitive endoderm. The AVE-specific expression of *Lim1* and *Hex1* appeared enlarged in *Oct1*-null embryos as compared with control littermates (Fig. 4A,B). By contrast, expression of the nascent mesoderm markers brachyury (*T*) and *Fgf8* was normal in *Oct1*-null embryos, except for the fact that it was displaced towards

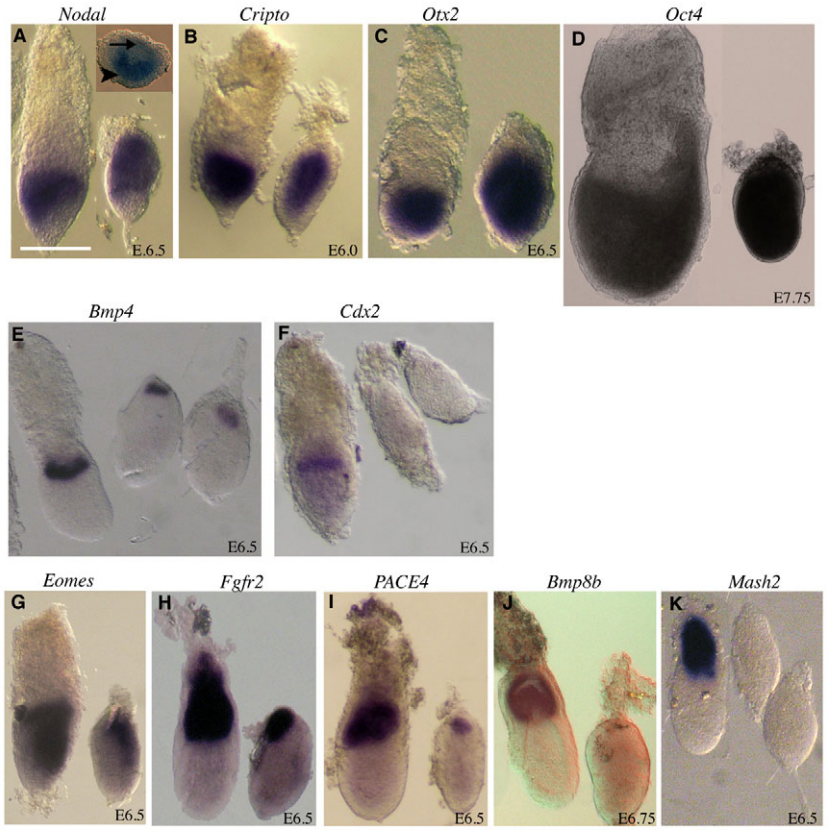

Fig. 3. *Oct1*-null embryos are defective in polar TE development. Whole-mount in situ hybridization of wild-type or *Oct1*-heterozygous (left in each panel) and *Oct1*-null (right) mouse embryos for markers of epiblast (EPI) (A-D), proximal extra-embryonic ectoderm (pExE) (E,F), ExE (G-J) and ectoplacental cone (EPC) (H,J,K). (**A**) *Nodal* is restricted to the proximal and the distal posterior of both wild-type and *Oct1*-null embryos at E6.5. The insert is a transverse section showing high posterior (arrowhead) and anterior (arrow) *Nodal* expression in the medial segment of the *Oct1* mutant embryo. (**B-D**) *Cripto*, *Otx2* and *Oct4* mark the EPI of wild-type or *Oct1*-heterozygous embryos, but their expression extends into the proximal edge of $Oct1^{-/-}$ embryos. (**E-J**) All analyzed pExE- and ExE-specific markers (*Bmp4*, *Cdx2*, *Eomes*, *Fgfr2* and *Pace4*), except for *Bmp8b* (J), are detected in a smaller domain of expression in $Oct1^{-/-}$ embryos than in wild-type or *Oct1*-heterozygous littermates. (**K**) *Mash2* is expressed in the EPC of wild-type embryos, whereas it is completely absent in $Oct1^{-/-}$ embryos. Scale bar: 150 μm.

the proximal end of the embryo (Fig. 4C,D). These data indicate that Oct1 deficiency does not impair specification of the A-P axis, but rather affects the induction magnitude of anterior polarity in the embryo.

Oct1 is required for the maintenance of TS cells

Since *Oct1*-null embryos contain a severely reduced ExE and lack the EPC, we reasoned that Oct1 might not be needed for EPI development but is necessary for proliferation and differentiation of the pTE-derived stem cell pool, both in vivo and in vitro (Chawengsaksophak et al., 1997; Russ et al., 2000).

TS cells can be isolated from E3.5 or E6.5 embryos cultured ex vivo in the presence of Fgf4 plus heparin and can be induced to differentiate by growth factor removal (Tanaka et al., 1998). We investigated *Oct1* expression in proliferating and differentiating TS cells. Oct1 and Cdx2 were co-expressed in undifferentiated TS cells (Fig. 5A). During trophoblast cell differentiation, the expression of the stem markers *Cdx2*, *Eomes* and *Essrb* was barely detectable as early as 3 days after Fgf4 withdrawal. However, only a minor downregulation of *Hand1* and *Oct1* transcripts was found in differentiated trophoblast cells even after 5 days of differentiation, indicating that Oct1 might be a pan-trophoblastic marker (Fig. 5B).

To test whether ICM-TE segregation occurs properly in pre-implantation embryos in the absence of Oct1, we performed qRT-PCR analysis of TE-specific and ICM-specific genes in blastocysts derived from *Oct1* heterozygous intercrossing. No significant changes in the expression of *Cdx2*, *Eomes*, *Fgfr2*, *Nanog* and *Oct4* were detected in any of the examined blastocysts, regardless of their genotype (see Fig. S2 in the supplementary material). This result suggests that either pTE specification does not require Oct1 or that the pTE is properly specified in the presence of maternal

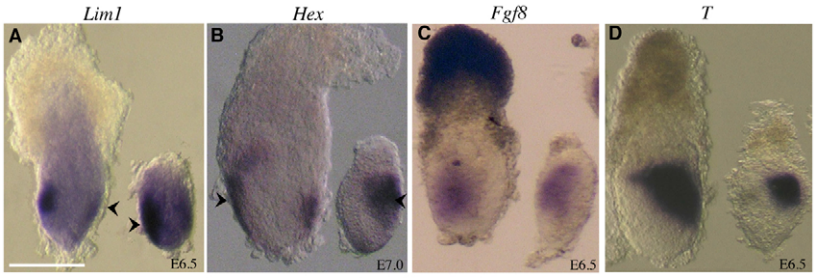

Fig. 4. *Oct1*-null mouse embryos possess an expanded AVE. Whole-mount in situ analysis of anterior visceral endoderm (AVE) (A,B) and primitive streak (PS) (C,D) markers at the indicated embryonic stage. (**A**,**B**) Anterior *Lim1* and *Hex* expression is found in a broader domain in *Oct1*-null than in wild-type embryos (left and right of each panel, respectively), indicating ectopic AVE formation in the absence of Oct1 (arrowheads indicate the anterior of the embryo). (**C**,**D**) PS specification is not impaired in *Oct1*-null embryos, as revealed by the proper posterior expression of the nascent mesoderm markers *Fgf8* and brachyury (*T*) at E6.5. Scale bar: 150 μm.

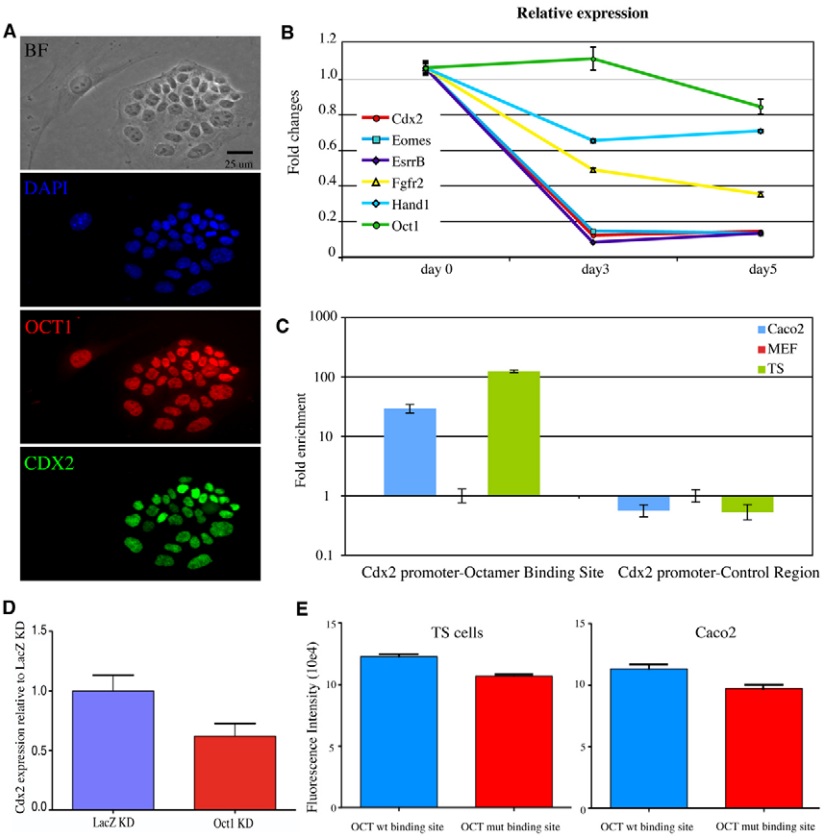

Fig. 5. Oct1 regulates *Cdx2* expression in mouse TS cells. (**A**) Immunofluorescence labeling of trophoblast stem (TS) colonies for Oct1 and Cdx2 showing co-localization of these factors in stem cells. Mouse embryonic fibroblast (MEF) cells express Oct1 only. (**B**) Expression analysis of trophoblast markers and Oct1 during differentiation of mouse TS cells cultured in the absence of Fgf4. (**C**) ChIP assay performed with an anti-Oct1 antibody on the *Cdx2* promoter region containing an octamer consensus sequence and on an unrelated region. Oct1 is enriched on the *Cdx2* proximal promoter in TS and human Caco2 cells, but not in MEFs. (**D**) *Cdx2* expression is downregulated in TS cells in which *Oct1* has been knocked down. *Cdx2* expression was normalized to levels detected in cells in which *lacZ* had been knocked down. (**E**) TS and Caco2 cells were infected with an Oct1-RFP expression construct in combination with either a wild-type octamer or a mutated octamer Cdx2-GFP expression vector, FACS sorted for RFP-GFP and assessed for GFP mean fluorescence intensity. GFP is decreased in cells infected with the reporter construct driven by the mutated octamer sequence.

Oct1. We therefore attempted to derive both ES and TS cells from pre-implantation *Oct1*-null embryos. *Oct1*-null ES lines were derived at the expected Mendelian ratio. These cells do not contain any Oct1 protein or binding activity, but continue to express SSEA-1 (Fut4 – Mouse Genome Informatics) and the pluripotency-associated markers Nanog and Oct4 (see Fig. S3 in the supplementary material). By contrast, of the 20 TS lines we derived from blastocysts obtained from *Oct1*-heterozygous intercrossing, 13 were heterozygous and the remaining seven were wild type. These results indicate that although Oct1 is dispensable for ES cell derivation, it is essential for the establishment or maintenance of pTE-derived stem cells in vitro. Moreover, they support the notion that Oct1 is required in vivo for the proliferation of ExE stem cells. However, it cannot be ruled out that Oct1 might be necessary for the differentiation of ExE TS cells as well.

We then tested the hypothesis that Oct1 might be involved in the regulation of *Cdx2* by binding to its promoter region, as previously shown for human cells of the intestinal epithelium (Jin and Li, 2001) and of the Caco2 colorectal adenocarcinoma line (Almeida et al., 2005). Sequence analysis of the mouse and human proximal *Cdx2* promoter revealed conservation of both the octamer canonical consensus and flanking regions (data not shown). ChIP assay performed with anti-Oct1 antibody showed a clear enrichment in the amplification of the region containing the octamer-binding consensus in comparison to the mock immunoprecipitation for both the human Caco2 and mouse TS samples (–116 and –154 bp relative to the transcription start site, respectively), but not for the MEF sample (P=0.0013) (Fig. 5C). In order to test whether *Oct1* regulates *Cdx2* transcription, we knocked down *Oct1* in TS cells using *Oct1*-specific shRNA. We observed downregulation of *Cdx2* expression following Oct1 downregulation (P<0.05; Fig. 5D). Additionally, mutation of the octamer binding site in the *Cdx2* promoter led to decreased expression of a GFP reporter gene in both Caco2 (P=0.0216) and TS (P=0.005) cells, as compared with expression from an unmutated *Cdx2* promoter (Fig. 5E). These results indicate that Oct1 specifically binds and regulates the *Cdx2* promoter region in murine TS cells as well as in human Caco2 cells.

Oct1 function is indispensable in the embryo proper

Our morphological and marker analyses showed that *Oct1*-null embryos are unable to develop beyond early gastrulation stages because of a failure in trophoblast development. However, as *Oct1* is expressed in embryonic tissues, the observed phenotype could also result from a combination of effects, i.e. from a lack of Oct1 in both the ExE and EPI. We set out to determine whether the gastrulation defect also occurred in embryos lacking Oct1 function solely in the EPI by performing a tetraploid complementation assay. Single wild-type 4-cell stage tetraploid embryos were aggregated to 8-cell stage diploid embryos derived from *Oct1* heterozygous intercrosses and allowed to develop to midgestation. None of the viable 35 chimaeric embryos recovered between E10.5 and E12.5 was *Oct1* null. At nominal stage E8.5, wild-type host ↔ Oct1-deficient chimeras were smaller than their littermates, but did not present any obvious morphological or developmental abnormalities. At E9.5, wild-type host ↔ *Oct1*-null chimeras were consistently growth retarded and developmentally arrested at neurula (headfold) stage with no more than four to five somites (E8.25) (Fig. 6), whereas heterozygous chimeric counterparts had clearly completed the turning process and displayed at least 16 somite pairs and a beating heart. These results suggest that Oct1 function in the embryonic tissues is not required for development from early to late gastrulation stages. They also indicate that Oct1

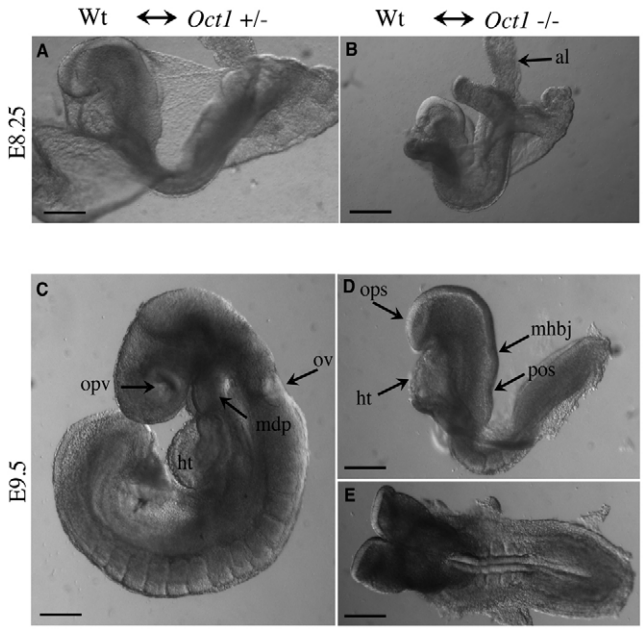

Fig. 6. Tetraploid aggregation chimeras composed of *Oct1*-null embryonic tissues are competent for development throughout all gastrulation stages. All analyzed chimeric mouse embryos contained wild-type extra-embryonic tissues and either *Oct1* wild-type or heterozygous (left of each panel) or null (right) EPI-derived tissues. (**A**,**B**) E8.25 chimeras composed of *Oct1*-null embryonic cells have reached the headfold stage, but are smaller than *Oct*-heterozygous chimeras. (**C-E**) At nominal stage E9.5, *Oct1*-heterozygous chimeras had completed the turning process and displayed 14-16 somite pairs, whereas *Oct1*-null chimeras, shown in lateral and dorsal view, were developmentally arrested at the early somite (4-5 pairs) stage corresponding to the headfold stage or E8.25. al, allantois; opv, optic vesicle; ov, otic vescicle; mdp, mandibular process; ht, heart; ops, optic sulcus; mhbj, mid-hindbrain junction; pos, pre-otic sulcus. Scale bars: 200 μm in A-C; 100 μm in D,E.

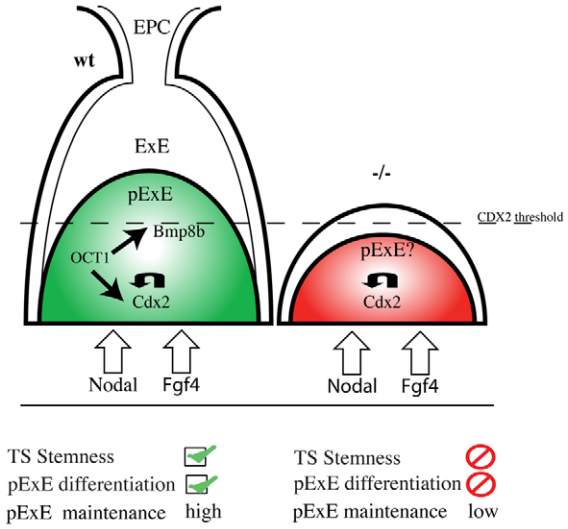

Fig. 7. Model of the role of Oct1 in the regulation of ExE development. During mouse post-implantation development, Oct1, together with other transcription factors, maintains levels of Cdx2 expression that are sufficient to ensure TS cell maintenance within the region of the ExE that is stimulated by Nodal and Fgf4 signaling (pExE). In *Oct1* mutant embryos, Cdx2 expression levels guarantee only limited TS maintenance within the pExE, resulting in a severe reduction of the ExE stem cell compartment. In addition, lack of Oct1 impairs the differentiation of pExE cells into the diploid precursor cells of both ExE and EPC. In vitro, lack of Oct1 activity is not compatible with the establishment of TS cell lines.

function is necessary in the embryo proper for normal development and/or growth to proceed from late gastrulation to the early somite stage.

DISCUSSION

In this study we describe the phenotype resulting from functional inactivation of the mouse *Oct1* locus and show that Oct1 plays a novel and unexpected role in TE development. Despite *OCT1* transcripts being detected in the human placenta and in some choriocarcinoma cell lines (Jimenez-Mateo et al., 2006), the expression and function of this factor in murine trophoblastic tissues have not been previously reported. *Oct1*-null embryos are unable to develop past the early streak stage, such that Oct1 deficiency leads to early embryonic death in utero, with all *Oct1*-null embryos dying by E9.5. Expression of the key molecular determinants of trophoblast fate, *Cdx2*, *Fgfr2* and *Eomes*, is normal in *Oct1*-null blastocysts, suggesting that either Oct1 does not take part in TE specification or that maternally inherited Oct1 (protein and/or transcript) is sufficient to sustain pre-implantation development. Additionally, *Oct1*-null embryos implant normally, indicating that the formation of primary giant cells, which mediate implantation by invading the uterine stroma and remodeling the maternal vasculature, is not affected by Oct1 deficiency. However, in utero histological examination of *Oct1* littermates at E6.75 revealed that *Oct1*-null embryos do not present an obvious embryonic or extra-embryonic polarity and lack an identifiable EPC, suggesting that ExE differentiation into EPC precursors is impaired by Oct1 loss. Our whole-mount ISH analysis of ExE and EPC markers at the early gastrulation stage, combined with the inability to derive *Oct1*-null TS cells, strongly indicate that both the expansion and differentiation of proliferative ExE TS cells require Oct1. Importantly, *Oct1*-null embryos contain a small ExE that lacks *Bmp8b* expression, suggesting not only that the size and molecular identity of the ExE are affected by Oct1 loss, but also that *Bmp8b* can be considered a direct or indirect Oct1 target in the proliferative ExE.

Previous studies showed that Elf5 and Erk2 (Mapk1 – Mouse Genome Informatics) are essential for TS cell self-renewal, as the ExE is totally absent in embryos deficient of either factor at E6.5. Moreover, TS cell lines could not be derived from *Elf5* and *Erk2* mutant embryos (Donnison et al., 2005; Saba-El-Leil et al., 2003). However, the presence of a small ExE in *Oct1*-null embryos suggests that Oct1 has a less stringent role than Elf5 and Erk2 in the maintenance of the proliferative capacity of ExE TS cells. Importantly, our data suggest that Oct1 deficiency is not permissive for the transition of proliferative ExE into ExE cells and EPC diploid precursors (Fig. 7). The absence of *Bmp8b* expression cannot account per se for these differentiation defects, as disruption of the *Bmp8b* locus does not have any effect on TE development (Ying and Zhao, 2000).

A candidate target of Oct1 in the ExE could be *Sox2*, which is expressed in both the EPI and the ExE of the early streak embryo (Avilion et al., 2003). Previous studies have highlighted the presence of multiple Oct binding sites within *Sox2* regulatory

regions (Catena et al., 2004; Tomioka et al., 2002). Although these studies have elucidated the capacity of the POU factors Oct4 and Brn1/Brn2 (Pou3f3/Pou3f2) to activate *Sox2* transcription in ES and neural cells, respectively, the identity of transcription factors regulating *Sox2* expression in the ExE has not yet been investigated. As *Oct1* is expressed in the ExE, it is possible that Oct1 might be important for driving *Sox2* expression in the ExE via the Oct sites.

The *Cdx2* promoter is autoregulated in cells that physiologically express Cdx2 (Xu et al., 1999), and Oct1 is an integral component of this autoregulatory loop, as mutation of the octamer binding site within the *Cdx2* proximal promoter interferes with both *Cdx2* expression and auto-activation. Autoregulation of the endogenous *Cdx2* gene has been observed in TS-like cells produced by inducible, enforced expression of a *Cdx2* transgene in ES cells (Tolkunova et al., 2006). Additionally, at stages later than blastocyst, Elf5 has been shown to reinforce *Cdx2* transcription via two binding sites located in the –780 to –184 region of the *Cdx2* promoter (Ng et al., 2008). In this study we present evidence that Oct1 interacts with the *Cdx2* promoter and regulates *Cdx2* transcription in mouse TS cells. We then propose that in proximal ExE cells stimulated by Fgf4 and Nodal, Oct1 might contribute to producing the threshold level of *Cdx2* transcription that triggers *Cdx2* autoregulation and ensures TS maintenance within the pExE (Fig. 7). Additionally, Oct1 is indispensable for pExE differentiation.

An exquisitely regulated network of interactions between the EPI and the ExE guarantees both ExE maintenance and the establishment of A-P polarity in the embryo. Nodal and Fgf signaling emanating from the EPI cooperate in maintaining ExE-specific expression of *Cdx2*, *Eomes* and *Esrrb* and in preventing precocious differentiation of the ExE (Brennan et al., 2001; Guzman-Ayala et al., 2004). Bmp4 signaling emanating from the ExE source mediates mesoderm formation by inducing *Wnt3* expression in the EPI, which in turn stimulates *T* and *Nodal* transcription (Ben-Haim et al., 2006; Liu et al., 1999). Translation of *Nodal* transcripts produces a pro-protein that must be processed in order to generate the fully active molecule. However, uncleaved Nodal can sustain extra-embryonic expression of its own convertases, *Pace4* and *Furin*, and of *Bmp4* (Ben-Haim et al., 2006).

Oct1 deficiency does not seem to have detrimental effects on *Nodal* transcription in E6.5-6.75 embryos. This result supports the conclusion that uncleaved-Nodal-dependent signaling acting on the ExE is intact in *Oct1*-null embryos. Additionally, we detected *T* and *Fgf8* expression on the posterior side of *Oct1*-null embryos at early gastrulation stage, whereas *Elf5*- and *Erk2*-null embryos do not show molecular signs of PS formation. This finding is consistent with the presence in *Oct1* mutants of an ExE remnant that still produces Bmp4 and Pace4 at the early streak stage. The expansion in AVE formation observed in the absence of Oct1 could be explained if *Oct1*-null embryos show lower levels, or a complete lack, of expression of the ExE-derived signaling molecule(s) that restrict DVE induction (Rodriguez et al., 2005). It has been proposed that Bmp8b, which is indeed absent from the *Oct1*-null ExE, might be such a signaling factor (Ohinata et al., 2009).

Based on our E6.5 analysis of embryonic markers, an Oct1 function that is restricted to the embryo proper is unlikely to contribute to the early streak arrest observed in *Oct1*-null embryos. Additionally, the gastrulation block of these embryos could be rescued by providing wild-type extra-embryonic tissues. However, because our tetraploid *Oct1*-null chimeric embryos are developmentally arrested at the early somite stage, we cannot rule out the possibility that the developmental arrest we have observed might have been slightly delayed by a contribution of wild-type cells to the embryo proper. Therefore, a systematic analysis of the differentiation capability of *Oct1*-null versus wild-type ES cells into all lineages both in vivo and in vitro is required to exactly pinpoint when Oct1 function in the embryonic tissues becomes necessary.

In conclusion, two POU factors play crucial roles during early embryogenesis in distinct tissues of the developing embryo. Oct4 is essential for ICM lineage specification (Nichols et al., 1998), whereas Oct1 primarily regulates ExE development. Further studies are needed to elucidate the modus operandi of Oct1 within the molecular network that underlies the proliferation and differentiation of the trophoblast lineages.

Acknowledgements

We thank Drs Richard Behringer, Daniel Constam, Jacqueline Deschamps, Brigid Hogan, K. Matsumoto, Janet Rossant and Michael Shen for kind gifts of whole-mount in situ probes; Dr Trono for pLVTHM and viral packaging plasmids; C. Ortmeier and M. Sinn for real-time PCR; and Patrick Kopp and Jean-François Spetz for ES cell work and generation of knockout mice. We are especially grateful to Michele Boiani for fruitful discussions, to Susanne Kölsch for editing the manuscript and to Peter Pfeffer and Tilo Kunath for critical reading of this manuscript. This work was supported by the Max Planck Society and the Novartis Research Foundation.

Competing interests statement

The authors declare no competing financial interests.

Supplementary material

Supplementary material for this article is available at
http://dev.biologists.org/lookup/suppl/doi:10.1242/dev.047027/-/DC1

References

Almeida, R., Almeida, J., Shoshkes, M., Mendes, N., Mesquita, P., Silva, E., Van Seuningen, I., Reis, C. A., Santos-Silva, F. and David, L. (2005). OCT-1 is over-expressed in intestinal metaplasia and intestinal gastric carcinomas and binds to, but does not transactivate, CDX2 in gastric cells. *J. Pathol.* **207**, 396-401.

Avilion, A. A., Nicolis, S. K., Pevny, L. H., Perez, L., Vivian, N. and Lovell-Badge, R. (2003). Multipotent cell lineages in early mouse development depend on SOX2 function. *Genes Dev.* **17**, 126-140.

Beck, F., Erler, T., Russell, A. and James, R. (1995). Expression of Cdx-2 in the mouse embryo and placenta: possible role in patterning of the extra-embryonic membranes. *Dev. Dyn.* **204**, 219-227.

Ben-Haim, N., Lu, C., Guzman-Ayala, M., Pescatore, L., Mesnard, D., Bischofberger, M., Naef, F., Robertson, E. J. and Constam, D. B. (2006). The nodal precursor acting via activin receptors induces mesoderm by maintaining a source of its convertases and BMP4. *Dev. Cell* **11**, 313-323.

Boiani, M., Eckardt, S., Leu, N. A., Scholer, H. R. and McLaughlin, K. J. (2003). Pluripotency deficit in clones overcome by clone-clone aggregation: epigenetic complementation? *EMBO J.* **22**, 5304-5312.

Brennan, J., Lu, C. C., Norris, D. P., Rodriguez, T. A., Beddington, R. S. and Robertson, E. J. (2001). Nodal signalling in the epiblast patterns the early mouse embryo. *Nature* **411**, 965-969.

Catena, R., Tiveron, C., Ronchi, A., Porta, S., Ferri, A., Tatangelo, L., Cavallaro, M., Favaro, R., Ottolenghi, S., Reinbold, R. et al. (2004). Conserved POU binding DNA sites in the Sox2 upstream enhancer regulate gene expression in embryonic and neural stem cells. *J. Biol. Chem.* **279**, 41846-41857.

Cavaleri, F. M., Balbach, S. T., Gentile, L., Jauch, A., Bohm-Steuer, B., Han, Y. M., Scholer, H. R. and Boiani, M. (2008). Subsets of cloned mouse embryos and their non-random relationship to development and nuclear reprogramming. *Mech. Dev.* **125**, 153-166.

Chawengsaksophak, K., James, R., Hammond, V. E., Kontgen, F. and Beck, F. (1997). Homeosis and intestinal tumours in Cdx2 mutant mice. *Nature* **386**, 84-87.

Cross, J. C., Flannery, M. L., Blanar, M. A., Steingrimsson, E., Jenkins, N. A., Copeland, N. G., Rutter, W. J. and Werb, Z. (1995). Hxt encodes a basic helix-loop-helix transcription factor that regulates trophoblast cell development. *Development* **121**, 2513-2523.

Ding, J., Yang, L., Yan, Y. T., Chen, A., Desai, N., Wynshaw-Boris, A. and Shen, M. M. (1998). Cripto is required for correct orientation of the anterior-posterior axis in the mouse embryo. *Nature* **395**, 702-707.
Donner, A. L., Episkopou, V. and Maas, R. L. (2007). Sox2 and Pou2f1 interact to control lens and olfactory placode development. *Dev. Biol.* **303**, 784-799.
Donnison, M., Beaton, A., Davey, H. W., Broadhurst, R., L'Huillier, P. and Pfeffer, P. L. (2005). Loss of the extraembryonic ectoderm in Elf5 mutants leads to defects in embryonic patterning. *Development* **132**, 2299-2308.
Eakin, G. S. and Hadjantonakis, A. K. (2006). Production of chimeras by aggregation of embryonic stem cells with diploid or tetraploid mouse embryos. *Nat. Protoc.* **1**, 1145-1153.
Erkman, L., McEvilly, R. J., Luo, L., Ryan, A. K., Hooshmand, F., O'Connell, S. M., Keithley, E. M., Rapaport, D. H., Ryan, A. F. and Rosenfeld, M. G. (1996). Role of transcription factors Brn-3.1 and Brn-3.2 in auditory and visual system development. *Nature* **381**, 603-606.
Guillemot, F., Nagy, A., Auerbach, A., Rossant, J. and Joyner, A. L. (1994). Essential role of Mash-2 in extraembryonic development. *Nature* **371**, 333-336.
Guzman-Ayala, M., Ben-Haim, N., Beck, S. and Constam, D. B. (2004). Nodal protein processing and fibroblast growth factor 4 synergize to maintain a trophoblast stem cell microenvironment. *Proc. Natl. Acad. Sci. USA* **101**, 15656-15660.
Haffner-Krausz, R., Gorivodsky, M., Chen, Y. and Lonai, P. (1999). Expression of Fgfr2 in the early mouse embryo indicates its involvement in preimplantation development. *Mech. Dev.* **85**, 167-172.
Hemberger, M., Nozaki, T., Masutani, M. and Cross, J. C. (2003). Differential expression of angiogenic and vasodilatory factors by invasive trophoblast giant cells depending on depth of invasion. *Dev. Dyn.* **227**, 185-191.
Hinkley, C. and Perry, M. (1992). Histone H2B gene transcription during Xenopus early development requires functional cooperation between proteins bound to the CCAAT and octamer motifs. *Mol. Cell. Biol.* **12**, 4400-4411.
Jaegle, M., Mandemakers, W., Broos, L., Zwart, R., Karis, A., Visser, P., Grosveld, F. and Meijer, D. (1996). The POU factor Oct-6 and Schwann cell differentiation. *Science* **273**, 507-510.
Jimenez-Mateo, O., Rodriguez-Torres, A., Avila, S. and Castrillo, J. L. (2006). The transcription factor PLA-1/SKN-1A is expressed in human placenta and regulates the placental lactogen-3 gene expression. *Placenta* **27**, 357-366.
Jin, T. and Li, H. (2001). Pou homeodomain protein OCT1 is implicated in the expression of the caudal-related homeobox gene Cdx-2. *J. Biol. Chem.* **276**, 14752-14758.
Johnson, L., Cao, X. and Jacobsen, S. (2002). Interplay between two epigenetic marks. DNA methylation and histone H3 lysine 9 methylation. *Curr. Biol.* **12**, 1360-1367.
Kehler, J., Tolkunova, E., Koschorz, B., Pesce, M., Gentile, L., Boiani, M., Lomeli, H., Nagy, A., McLaughlin, K. J., Scholer, H. R. et al. (2004). Oct4 is required for primordial germ cell survival. *EMBO Rep.* **5**, 1078-1083.
Lawson, K. A., Dunn, N. R., Roelen, B. A., Zeinstra, L. M., Davis, A. M., Wright, C. V., Korving, J. P. and Hogan, B. L. (1999). Bmp4 is required for the generation of primordial germ cells in the mouse embryo. *Genes Dev.* **13**, 424-436.
Liu, P., Wakamiya, M., Shea, M. J., Albrecht, U., Behringer, R. R. and Bradley, A. (1999). Requirement for Wnt3 in vertebrate axis formation. *Nat. Genet.* **22**, 361-365.
Luo, J., Sladek, R., Bader, J. A., Matthyssen, A., Rossant, J. and Giguere, V. (1997). Placental abnormalities in mouse embryos lacking the orphan nuclear receptor ERR-beta. *Nature* **388**, 778-782.
Mason, J. O., Williams, G. T. and Neuberger, M. S. (1985). Transcription cell type specificity is conferred by an immunoglobulin VH gene promoter that includes a functional consensus sequence. *Cell* **41**, 479-487.
Muller, M. M., Ruppert, S., Schaffner, W. and Matthias, P. (1988). A cloned octamer transcription factor stimulates transcription from lymphoid-specific promoters in non-B cells. *Nature* **336**, 544-551.
Ng, R. K., Dean, W., Dawson, C., Lucifero, D., Madeja, Z., Reik, W. and Hemberger, M. (2008). Epigenetic restriction of embryonic cell lineage fate by methylation of Elf5. *Nat. Cell Biol.* **10**, 1280-1290.
Nichols, J., Zevnik, B., Anastassiadis, K., Niwa, H., Klewe-Nebenius, D., Chambers, I., Scholer, H. and Smith, A. (1998). Formation of pluripotent stem cells in the mammalian embryo depends on the POU transcription factor Oct4. *Cell* **95**, 379-391.
Ohinata, Y., Ohta, H., Shigeta, M., Yamanaka, K., Wakayama, T. and Saitou, M. (2009). A signaling principle for the specification of the germ cell lineage in mice. *Cell* **137**, 571-584.
Phillips, K. and Luisi, B. (2000). The virtuoso of versatility: POU proteins that flex to fit. *J. Mol. Biol.* **302**, 1023-1039.
Pomerantz, J. L. and Sharp, P. A. (1994). Homeodomain determinants of major groove recognition. *Biochemistry* **33**, 10851-10858.
Rodriguez, T. A., Srinivas, S., Clements, M. P., Smith, J. C. and Beddington, R. S. (2005). Induction and migration of the anterior visceral endoderm is regulated by the extra-embryonic ectoderm. *Development* **132**, 2513-2520.
Russ, A. P., Wattler, S., Colledge, W. H., Aparicio, S. A., Carlton, M. B., Pearce, J. J., Barton, S. C., Surani, M. A., Ryan, K., Nehls, M. C. et al. (2000). Eomesodermin is required for mouse trophoblast development and mesoderm formation. *Nature* **404**, 95-99.
Saba-El-Leil, M. K., Vella, F. D., Vernay, B., Voisin, L., Chen, L., Labrecque, N., Ang, S. L. and Meloche, S. (2003). An essential function of the mitogen-activated protein kinase Erk2 in mouse trophoblast development. *EMBO Rep.* **4**, 964-968.
Sauter, P. and Matthias, P. (1998). Coactivator OBF-1 makes selective contacts with both the POU-specific domain and the POU homeodomain and acts as a molecular clamp on DNA. *Mol. Cell. Biol.* **18**, 7397-7409.
Scheidereit, C., Heguy, A. and Roeder, R. G. (1987). Identification and purification of a human lymphoid-specific octamer-binding protein (OTF-2) that activates transcription of an immunoglobulin promoter in vitro. *Cell* **51**, 783-793.
Scholer, H. R. (1991). Octamania: the POU factors in murine development. *Trends Genet.* **7**, 323-329.
Segil, N., Roberts, S. B. and Heintz, N. (1991). Mitotic phosphorylation of the Oct-1 homeodomain and regulation of Oct-1 DNA binding activity. *Science* **254**, 1814-1816.
Shakya, A., Cooksey, R., Cox, J. E., Wang, V., McClain, D. A. and Tantin, D. (2009). Oct1 loss of function induces a coordinate metabolic shift that opposes tumorigenicity. *Nat. Cell Biol.* **11**, 320-327.
Strubin, M., Newell, J. W. and Matthias, P. (1995). OBF-1, a novel B cell-specific coactivator that stimulates immunoglobulin promoter activity through association with octamer-binding proteins. *Cell* **80**, 497-506.
Strumpf, D., Mao, C. A., Yamanaka, Y., Ralston, A., Chawengsaksophak, K., Beck, F. and Rossant, J. (2005). Cdx2 is required for correct cell fate specification and differentiation of trophectoderm in the mouse blastocyst. *Development* **132**, 2093-2102.
Tam, P. P., Loebel, D. A. and Tanaka, S. S. (2006). Building the mouse gastrula: signals, asymmetry and lineages. *Curr. Opin. Genet. Dev.* **16**, 419-425.
Tanaka, S., Kunath, T., Hadjantonakis, A. K., Nagy, A. and Rossant, J. (1998). Promotion of trophoblast stem cell proliferation by FGF4. *Science* **282**, 2072-2075.
Tantin, D., Schild-Poulter, C., Wang, V., Hache, R. J. and Sharp, P. A. (2005). The octamer binding transcription factor Oct-1 is a stress sensor. *Cancer Res.* **65**, 10750-10758.
Thisse, B. and Thisse, C. (2005). Functions and regulations of fibroblast growth factor signaling during embryonic development. *Dev. Biol.* **287**, 390-402.
Thomas, P. Q., Brown, A. and Beddington, R. S. (1998). Hex: a homeobox gene revealing peri-implantation asymmetry in the mouse embryo and an early transient marker of endothelial cell precursors. *Development* **125**, 85-94.
Tolkunova, E., Cavaleri, F., Eckardt, S., Reinbold, R., Christenson, L. K., Scholer, H. R. and Tomilin, A. (2006). The caudal-related protein cdx2 promotes trophoblast differentiation of mouse embryonic stem cells. *Stem Cells* **24**, 139-144.
Tomioka, M., Nishimoto, M., Miyagi, S., Katayanagi, T., Fukui, N., Niwa, H., Muramatsu, M. and Okuda, A. (2002). Identification of Sox-2 regulatory region which is under the control of Oct-3/4-Sox-2 complex. *Nucleic Acids Res.* **30**, 3202-3213.
Tsang, T. E., Shawlot, W., Kinder, S. J., Kobayashi, A., Kwan, K. M., Schughart, K., Kania, A., Jessell, T. M., Behringer, R. R. and Tam, P. P. (2000). Lim1 activity is required for intermediate mesoderm differentiation in the mouse embryo. *Dev. Biol.* **223**, 77-90.
Uy, G. D., Downs, K. M. and Gardner, R. L. (2002). Inhibition of trophoblast stem cell potential in chorionic ectoderm coincides with occlusion of the ectoplacental cavity in the mouse. *Development* **129**, 3913-3924.
Veenstra, G. J., van der Vliet, P. C. and Destree, O. H. (1997). POU domain transcription factors in embryonic development. *Mol. Biol. Rep.* **24**, 139-155.
Verrijzer, C. P., Alkema, M. J., van Weperen, W. W., Van Leeuwen, H. C., Strating, M. J. and van der Vliet, P. C. (1992). The DNA binding specificity of the bipartite POU domain and its subdomains. *EMBO J.* **11**, 4993-5003.
Wang, V. E., Schmidt, T., Chen, J., Sharp, P. A. and Tantin, D. (2004). Embryonic lethality, decreased erythropoiesis, and defective octamer-dependent promoter activation in Oct-1-deficient mice. *Mol. Cell. Biol.* **24**, 1022-1032.
Xu, F., Li, H. and Jin, T. (1999). Cell type-specific autoregulation of the Caudal-related homeobox gene Cdx-2/3. *J. Biol. Chem.* **274**, 34310-34316.
Yang, J., Muller-Immergluck, M. M., Seipel, K., Janson, L., Westin, G., Schaffner, W. and Pettersson, U. (1991). Both Oct-1 and Oct-2A contain domains which can activate the ubiquitously expressed U2 snRNA genes. *EMBO J.* **10**, 2291-2296.
Ying, Y. and Zhao, G. Q. (2000). Detection of multiple bone morphogenetic protein messenger ribonucleic acids and their signal transducer, Smad1, during mouse decidualization. *Biol. Reprod.* **63**, 1781-1786.
Zeller, R., Rogers, M., Haramis, A. G. and Carrasceo, A. S. (2001). In situ hybridization to cellular RNA. *Curr. Protoc. Mol. Biol.* **14**, Unit 14.3.
Zhao, F. Q., Zheng, Y., Dong, B. and Oka, T. (2004). Cloning, genomic organization, expression, and effect on beta-casein promoter activity of a novel isoform of the mouse Oct-1 transcription factor. *Gene* **326**, 175-187.